

Thermal Conductivity of Electron-Irradiated CdS[†]

Frederick L. Vook

Sandia Laboratories, Albuquerque, New Mexico 87115

(Received 15 October 1970)

Measurements were made of the change in low-temperature thermal conductivity of high-resistivity sulfur-compensated single-crystal CdS upon electron irradiation and annealing. Samples oriented parallel and perpendicular to the hexagonal c axis of CdS were irradiated with 2-MeV electrons below 25 °K to fluences Φ totaling 7.8×10^{17} electrons/cm². The increase in the additive thermal resistivity at 11 °K on irradiation was found to be independent of the orientation of the sample, and $1/K - 1/K_0 = (5.5 \times 10^{-10}) \Phi^{0.5}$ cm deg/W. Isochronal annealing measurements show almost complete annealing out of the additive thermal resistivity below room temperature, and recovery begins as low as 35 °K. There are three major annealing stages centered near 45, 75, and 225 °K. Annealing above 60 °K produces an anisotropic thermal conductivity for subsequent measurements below 20 °K. The anisotropic additive thermal resistivity is much greater if the temperature gradient is perpendicular to the c axis than if it is parallel. The anisotropic phonon scattering is attributed to the formation and temperature-dependent orientation of anisotropic defects. It is concluded that the defect orientation parallel to the c axis has the lowest energy, and measurements of the temperature dependence of the thermal conductivity parallel and perpendicular to the c axis give the equilibrium energy difference for reorientation to be $\approx 1.5 \times 10^{-3}$ eV.

I. INTRODUCTION

Studies of radiation effects in elemental and compound semiconductors have shown that primary defects move at very low temperature,¹ and it would be surprising if this were not also the case in CdS. However, the migration energies and migration temperatures of the simple primary defects in CdS have not yet been determined. If primary defects introduced into CdS move and interact with impurities or stoichiometric defects well below room temperature, it may be expected that many of the room-temperature stable defects are defect complexes. Primary defects must, therefore, be studied in high-purity CdS, irradiated and measured at low temperatures. A few CdS investigations have been made for irradiations near liquid-nitrogen temperature, but extensive annealing measurements have not been reported.

Much of the research in CdS has been devoted to the study of mechanisms of luminescence and the nature of the luminescent centers.²⁻⁹ Although the identity and structure of the defects responsible for the various emission bands remain unclear, luminescence measurements have been used in electron-energy-damage threshold experiments to infer the displacement of the constituent atoms. Collins⁶ observed the production of edge emission (5200 Å) by 200-keV electron bombardment at liquid-nitrogen temperature. Kulp and Kelley⁷ subsequently measured the room-temperature threshold for the production of edge emission to be 115 keV and attributed this threshold to the transfer of 8.7 eV to the sulfur atom. Kulp⁸ found a second higher threshold at 290

keV and attributed this threshold to the transfer of 7.3 eV to a cadmium atom. Kulp further showed that the fluorescences produced by electron bombardment at 85 °K recovered considerably, but often not completely, upon heating to room temperature and cooling again. No interpretation of the annealing was made.

Bryant and Cox⁹ measured the electron-energy-damage threshold at 77 °K for the production of a cathodoluminescence band. They found the electron-energy threshold to be 125 keV and attributed this threshold to the transfer of 9.6 eV to a sulfur atom. They concluded that this was the same threshold that Kulp and Kelley reported to be 8.7 eV for sulfur displacement at room temperature. The damage was reported to thermally anneal out between liquid-nitrogen temperature and room temperature, but more detailed annealing measurements were not made. However, significant radiation annealing was noted to occur during irradiation at liquid-nitrogen temperature.

Chester¹⁰ made room-temperature irradiations of CdS with ⁶⁰Co and ¹³⁷Cs γ rays. A few ⁶⁰Co γ irradiations were made at liquid-nitrogen temperature, but the damage as observed by electrical measurements was not significantly different from that produced at room temperature. Furthermore, no recovery of the damage was observed upon warming the sample to room temperature. The lack of recovery between liquid-nitrogen and room temperature observed by Chester is surprising. It is important to determine whether this occurred because primary defects migrated at low temperature to form defect complexes which were stable upon an-

nealing to room temperature.

In the present paper,¹¹ low-temperature thermal-conductivity measurements were used to investigate primary defects introduced by electron irradiation in CdS at temperatures below 25 °K. Low-temperature thermal conductivity has been shown to be highly sensitive to lattice defects introduced by electron irradiation into high-purity GaAs,¹² InSb,¹³ Ge,¹⁴ and Si.¹⁵ The increase in low-temperature thermal resistivity on electron irradiation can be related to theories of phonon scattering, and the magnitude and kind of such scattering can differ greatly from one semiconductor to another. It has also been shown¹² that changes in the temperature dependence of the low-temperature thermal conductivity on annealing are related to changes in the structural properties of the defects and are therefore useful in distinguishing between different kinds of radiation-induced defects.

Since CdS has the hexagonal crystal structure it is also possible with thermal-conductivity measurements to determine whether an anisotropy in the phonon scattering of the induced defects occurs and whether it can be related to the formation of anisotropic defects. Fortunately, experimental measurements have shown that the thermal conductivity of pure CdS is isotropic.¹⁶ For these reasons, changes in the thermal conductivity of electron-irradiated CdS were used as tools to investigate the production, annealing, and anisotropy of primary defects produced in CdS at temperatures below 25 °K.

Following a description of the experiments and presentation of the results, the phonon scattering of the defects introduced by electron irradiation in CdS is compared with theories and experimental measurements of the scattering introduced by electron irradiation in other semiconductors. The temperature dependence of the thermal conductivity below annealing temperatures is used to deduce the low-temperature formation of anisotropic defects whose phonon scattering strongly depends on their orientation with respect to the temperature gradient. Finally, the annealing measurements of the thermal conductivity are compared with other measurements of annealing in electron-irradiated CdS, and models for the low-temperature motion of primary defects in CdS are proposed.

II. EXPERIMENTAL

Measurements of the change in thermal conductivity of high-purity single-crystal CdS were made *in situ* without warm up at a base temperature near 10 °K. The experimental arrangement and measuring apparatus were similar to those reported in preceding papers. Two samples were irradiated simultaneously and then annealed together. As

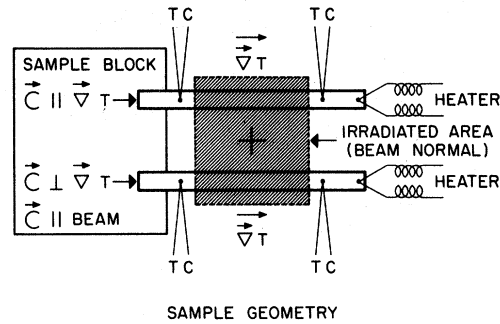


FIG. 1. Schematic diagram of the sample geometry indicating the orientation of the samples relative to the c axis and temperature gradient. Top, CdS- $c||$. Bottom, CdS- $c\perp$.

shown in Fig. 1, each sample was soldered at one end to a sample block which in turn was conduction cooled in an irradiation cryostat. Measurements of the change in thermal conductivity were made using small wire heaters attached to the ends of the samples. Thermal-conductivity measurements were made as a function of the 2-MeV electron fluence and as a function of the annealing temperature following irradiation. The fraction of the heater power which flowed through a sample was obtained by calibration of the heater using measurements of the thermal conductivity parallel to the c axis of unirradiated CdS at 300 °K given by Holland.¹⁷ Chromel P vs constantan thermocouples were used for the temperature measurements.

Two essentially equivalent samples, CdS- $c||$ and CdS- $c\perp$, were prepared from high-purity single-crystal material (obtained from Clevite Corp). CdS crystals as grown are initially highly conductive n type because of nonstoichiometry or foreign donors; and high-resistivity crystals are made by annealing in a sulfur-containing atmosphere, where native acceptors, presumably Cd vacancies, compensate the donors. The crystals as received were high-resistivity sulfur-compensated crystals which exhibited near-edge emission. The unirradiated photoelectronic properties of crystals from the same slices as CdS- $c||$ and CdS- $c\perp$ and the photoelectronic properties of CdS- $c||$ and CdS- $c\perp$ after irradiation and warming to room temperature were also investigated and reported by Im and Bube.¹⁸ Both samples CdS- $c||$ and CdS- $c\perp$ were bar shaped and were, respectively, 0.136 and 0.138 cm wide, 0.049 and 0.047 cm thick with irradiated lengths of 1.0 cm. The samples were oriented as shown in Fig. 1 so that for CdS- $c||$ the long dimension of the crystal and temperature gradient were parallel to the c axis; whereas for CdS- $c\perp$, the c axis was perpendicular to the long dimension of the crystal and temperature gradient.

During irradiations, the base temperature of the

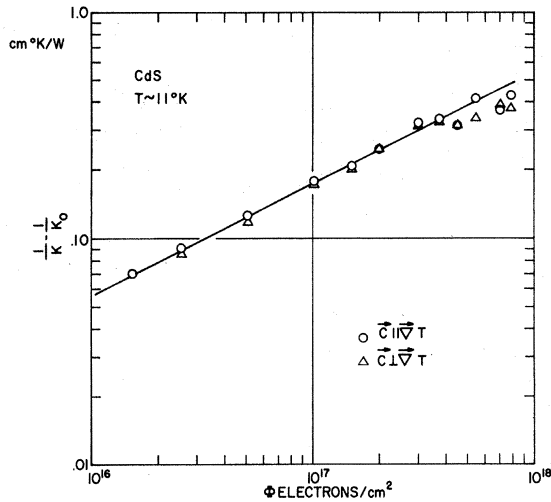


FIG. 2. Increase in the additive thermal resistivity near 11 °K as a function of the fluence of incident 2.0-MeV electrons.

samples was near 10 °K. The samples were irradiated with such a flux that the maximum temperature of the sample tip was never more than 25 °K. Measurements of the increase in thermal resistivity were made periodically on irradiation using the sample heater. After a total fluence of 7.8×10^{17} (2-MeV electrons/cm²) was reached, 15-min isochronal anneals were performed in steps to 300 °K. In addition, the temperature dependence of the thermal conductivity was measured before irradiation and below the annealing temperatures for selected anneal temperatures.

III. RESULTS

The data from CdS-*c*|| and CdS-*c*⊥ agree very well with each other on bombardment, but differ considerably upon annealing. It will be shown later that the difference upon annealing is attributed to the difference in the orientation of the *c* axis with respect to the temperature gradient for the two crystals. The increase in the additive thermal resistivity at 11 °K on bombardment is shown in Fig. 2. The thermal-resistivity increase is a non-linear function of the electron fluence Φ and is nearly proportional to the 0.5 power. The data for both samples at 11 °K can be fitted closely by $1/K - 1/K_0 = (5.5 \times 10^{-10})\Phi^{0.5}$ cm deg/W.

Figure 3 shows normalized measurements of thermal resistivity $W \equiv 1/K$ as a function of annealing temperature for 15-min isochronal anneals with all measurements made near 12 °K. W_0 and W_M are the thermal resistivities at 12 °K at the beginning and end of the irradiation, respectively. It can be seen that the thermal-resistivity annealing, as measured at 12 °K, is quite different for CdS-*c*⊥ where the *c* axis is perpendicular to the

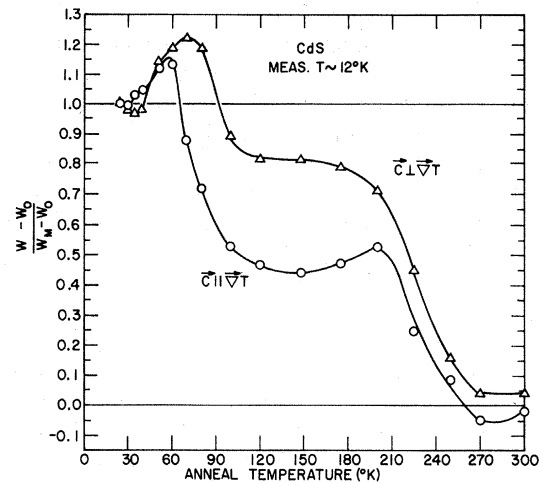


FIG. 3. Fraction of the additive thermal resistivity at 12 °K that remains after successive 15-min anneals. Measurements made at 12 °K after each anneal and plotted at the anneal temperature.

temperature gradient compared with CdS-*c*|| where the *c* axis is parallel to the temperature gradient. Since the recovery behavior is quite different for these two samples even though the changes on bombardment were the same, the unrecovered fraction of the additive thermal resistivity $(W - W_0)/(W_M - W_0)$ is not necessarily directly proportional to the fraction of damage remaining.

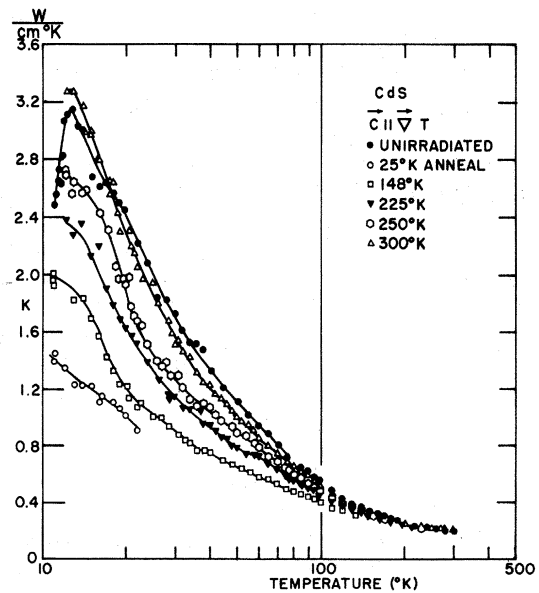


FIG. 4. Temperature dependence of the thermal conductivity of CdS-*c*|| before irradiation and after irradiation below each of the indicated 15-min anneal temperatures.

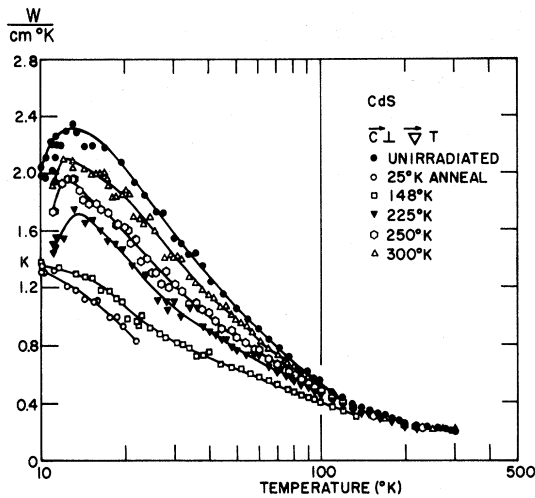


FIG. 5. Temperature dependence of the thermal conductivity of CdS-c \perp before irradiation and after irradiation below each of the indicated 15-min anneal temperatures.

It is observed that the thermal resistivity exhibits recovery beginning near 35 °K, and that almost complete recovery of the additive thermal resistivity occurs below 300 °K. Reverse recovery stages appear near 45 °K in both samples, and major recovery stages begin in both samples near 60 and 175 °K. It should also be noted that for the sample where the c axis is parallel to the temperature gradient, annealing to 300 °K apparently removed all the additive thermal resistivity, and, in fact, the thermal resistivity at 12 °K of the irradiated and annealed sample is *less* than the thermal resistivity at this temperature in the unirradiated sample.

Figure 4 shows the temperature dependence of

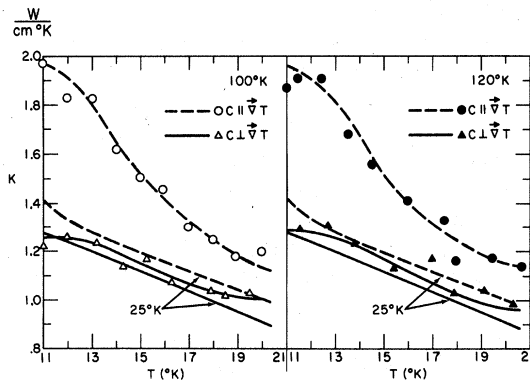


FIG. 6. Comparison of the temperature dependence of the thermal conductivity of CdS-c \parallel and CdS-c \perp after 15-min annealing at 100 and 120 °K. Curves are shown for the thermal conductivity after 25 °K anneals for comparison.

the thermal conductivity of CdS-c \parallel before irradiation and after irradiation below the indicated anneal temperatures. Note again that the thermal conductivity at 12 °K after low-temperature irradiation followed by annealing to 300 °K is larger than in the unirradiated sample. Figure 5 shows the corresponding results for CdS-c \perp . Additional temperature-dependence studies were made below other anneal temperatures, but these are not shown in Figs. 4 and 5 to preserve clarity. In contrast to results of electron irradiation on the thermal conductivity of other semiconductors,¹²⁻¹⁴ the results in Figs. 4 and 5 do not show large shifts in the thermal-conductivity maximum to higher temperatures following bombardment.

Figures 6 and 7 show additional temperature-dependence results in more detail for the two samples below anneal temperatures of 100, 125, 148, and 175 °K. The curves for the 25 °K anneals are also shown for comparison. It can be seen that for annealing above 100 °K the recovery of the thermal conductivity for the sample with the c axis parallel to the temperature gradient is much greater than for the sample with the c axis perpendicular to the temperature gradient. Although the results seem to be quite different for the two samples, they will be interpreted quite simply to arise from measurements of the properties of the same number and kinds of defects formed in both samples.

IV. DISCUSSION

A. Bombardment

The thermal conductivity of CdS is lattice thermal conductivity since the electrical conductivity is so small. The samples studied here were high-purity and high-dark-resistivity samples. They remain high-resistivity after irradiation as indicated in Table I, which gives the results of the photoelectron-

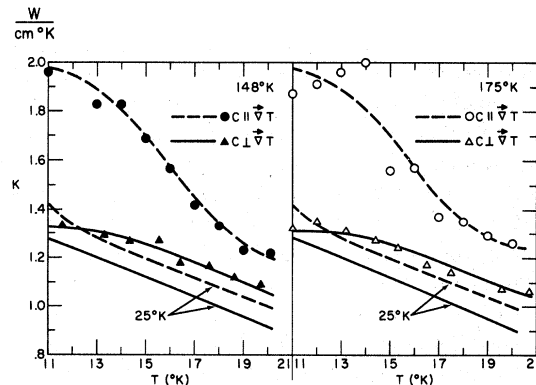


FIG. 7. Comparison of the temperature dependence of the thermal conductivity of CdS-c \parallel and CdS-c \perp after 15-min annealing at 148 and 175 °K. Curves are shown for the thermal conductivity after 25 °K anneals for comparison.

TABLE I. Photoelectronic measurements of Im and Bube (Ref. 18).

Measured quantity	c_{11} major plane Material of CdS-c		c_1 major plane Material of CdS-cl		CdS-c	CdS-cl
	Un-irradiated	10^{16} (2-MeV electrons/cm ²)	Un-irradiated	10^{17} (2-MeV electrons/cm ²)	7.85×10^{17} (2-MeV electrons/cm ²)	7.85×10^{17} (2-MeV electrons/cm ²)
Dark conductivity, 330 °K (Ω cm) ⁻¹	7×10^{-11}	6×10^{-11}	2×10^{-10}	10^{-9}	7×10^{-9}	7×10^{-9}
Dark conductivity, activation energy (eV)	0.68	0.69	0.74	0.69	0.63	0.64
Variation in Fermi level between 296 and 370 °K	0.75-0.77	0.75-0.77	0.73-0.75	0.69-0.69
Electron lifetime (msec)	2.95	0.036?	1.19	0.15	0.29	0.30
Ratio of quenching at 1.4 μ to that in 0.9- μ region			0.33	0.70
Electron cross section of sensitizing centers (cm ²)	8×10^{-22}	10^{-20}	5×10^{-21}	5×10^{-21}

ic measurements of Im and Bube.¹⁸ The principal photoelectronic effect remaining after low-temperature irradiation and annealing to room temperature is a decrease in the electron lifetime.

As shown in Fig. 2, the additive thermal resistivity is approximately proportional to the square root of the fluence of 2-MeV electrons. The same dependence on defect concentration is also implied, assuming a constant introduction rate of defects. The 0.5 power dependence of $1/K - 1/K_0$ observed for 2-MeV electron-irradiated CdS is very similar to the 0.58 power dependence observed for electron-irradiated germanium,¹⁴ and the 0.61 power dependence observed for electron-irradiated silicon.¹⁵ Theoretical studies to explain the magnitude and defect-concentration dependence of thermal scattering have been made by several authors and previously reviewed.^{12, 14} Most older theories predict that the additive thermal resistivity is directly proportional to the concentration of defects for small concentrations. At high concentrations, several theories have predicted that the defect thermal resistivity is proportional to the square root of the concentration as is observed here for CdS.

Recently, the first attempt to rigorously calculate the thermal conductivity of a finite dielectric crystal containing defects was undertaken by Erdős.¹⁹ Erdős solved the Boltzmann transport equation exactly for a finite insulator with small temperature gradient and random scattering centers. He found that for the Rayleigh scattering of phonons by point defects in the strong-scattering limit, the thermal resistivity is explicitly proportional to the $\frac{3}{4}$ power

of the impurity concentration. This surprising result was interpreted as a demonstration of the cooperative nature of the impurity scattering.

A more recent second attempt to rigorously calculate the thermal conductivity of a finite dielectric crystal containing defects has been given by Kazakov and Nagaev²⁰ for the nonlinear problem of a system arbitrarily far from equilibrium. In the limit of strong scattering of phonons by point defects, both treatments predict that the thermal resistivity is explicitly proportional to the $\frac{3}{4}$ power of the impurity concentration, and in the weak scattering limit, that the thermal conductivity decreases by a term directly proportional to the concentration of defects. Experimental observation of the $\frac{3}{4}$ -power concentration dependence has been presented¹³ in the results of the very strong phonon scattering produced in electron-irradiated InSb.

In summary, many experimental studies of the changes in the thermal conductivity of semiconductors upon electron irradiation have shown that for a particular semiconductor, the additive thermal resistivity increases as a constant fractional power (≤ 1) of the defect concentration.^{12-15, 21} The reasons that this rule is obeyed and that the fractional power is different for different semiconductors are not completely clear, although recent theoretical studies^{19, 20} show that other than linear dependences are to be expected.

B. Anisotropic Thermal Conductivity

Although the increase in the thermal resistivity on bombardment below 25 °K is independent of the

orientation of the sample as shown in Fig. 2, the additive thermal resistivity no longer remains isotropic after annealing as shown in Fig. 3. These results imply that the recovery of the primary defects introduced on irradiation is not simply a recombination of interstitials with their respective vacancies. To the knowledge of the author, the only other example of an anisotropic thermal scattering of defects in crystals is given by dislocation scattering in CaF_2 .²²

Since the anisotropy becomes greatest upon annealing near 100 to 200 °K, it is important to examine the temperature dependence of the thermal conductivity of the two samples after annealing in this temperature region. These results are shown in Figs. 4–7. For the 148 °K anneal in Figs. 4 and 7, a sharp rise in thermal conductivity with decreasing temperature is evident below 20 °K in the sample in which the c axis is parallel to the temperature gradient. In contrast, the thermal conductivity below 20 °K for the sample with the c axis perpendicular to the temperature gradient (Figs. 5 and 7) rises very slowly, and near 10 °K is still very near to the value observed after bombardment. Similar differences are shown in detail in Figs. 6 and 7 for the 100, 200, 148, and 175 °K anneals.

Upon bombardment at irradiation temperatures below 25 °K it is proposed that isolated immobile and randomly dispersed interstitial- and vacancy-type defects are produced. Consequently, the additive thermal resistivity is isotropic and equal in the two samples. However, upon annealing the resulting anisotropy in the thermal conductivity is attributed to the formation and temperature-dependent angular distribution of anisotropic defects whose phonon scattering is a strong function of their orientation with respect to the temperature gradient. Since the thermal conductivity is largest at low temperature when the temperature gradient lies along the c axis, we take this to imply that the lowest-energy position for these anisotropic defects is along the c axis. At very low temperatures, the anisotropic defects line up parallel to the c axis, and as the measuring temperature is raised the anisotropy in the thermal conductivity decreases as the anisotropic defects begin to thermally reorient and finally become randomly oriented in the crystal.

Figure 3 suggests that the anisotropic defects dominate the additive thermal resistivity for anneal temperatures ≥ 100 °K. If the anisotropic defects dominate the additive thermal resistivity, measurements for the two samples of the temperature dependence of the additive thermal resistivity $1/K - 1/K_0$ parallel and perpendicular to the c axis can be used to determine the equilibrium energy difference of rotation of the defects ΔE and

$$1/K - 1/K_0 = A_{\perp \nabla T} N_{\perp \nabla T} + A_{\parallel \nabla T} N_{\parallel \nabla T} \approx A_{\perp \nabla T} N_{\perp \nabla T},$$

assuming $A_{\perp \nabla T} \gg A_{\parallel \nabla T}$,

where $N_{\perp \nabla T}$ is the number of anisotropic defects aligned perpendicular to the temperature gradient $\vec{\nabla}T$, $N_{\parallel \nabla T}$ is the number of anisotropic defects aligned parallel to the temperature gradient, and $A_{\perp \nabla T}$ and $A_{\parallel \nabla T}$ are the corresponding coefficients of the scattering. If we define R as the ratio of the additive thermal resistivity for the sample in which \vec{c} is perpendicular to $\vec{\nabla}T$ to the additive thermal resistivity for the sample in which \vec{c} is parallel to $\vec{\nabla}T$, then for a Boltzmann distribution, we have

$$R \equiv \frac{(1/K - 1/K_0)_{\perp \nabla T}}{(1/K - 1/K_0)_{\parallel \nabla T}} = \frac{(N_{\perp \nabla T})_{\perp \nabla T}}{(N_{\perp \nabla T})_{\parallel \nabla T}} \approx \frac{N_{\parallel c}}{N_{\perp c}} \propto e^{\Delta E/kT},$$

where $N_{\parallel c}$ and $N_{\perp c}$ are the number of anisotropic defects parallel and perpendicular to the c axis, respectively. Figure 8 gives results of the logarithm of this ratio as a function of reciprocal measuring temperature for the curves shown in Figs. 4–7 after annealing to the indicated anneal temperatures between 100 and 175 °K. The measurements give an energy difference of $\Delta E = 1.5 \times 10^{-3}$ eV, which is equal to kT at ~ 17 °K.

Since this analysis successfully explains the orientation dependence of the thermal conductivity, we may extend it to determine the annealing temperature at which the anisotropic defects form. From Fig. 3 we may anticipate that this temperature is near 60 °K. Figure 9 gives the logarithm of R vs reciprocal measuring temperature for anneal temperatures between 25 and 80 °K. The points on the curves on Fig. 9 are not data points but are obtained from smoothed curves of the data. We see that for anneal temperatures of 60 °K and below,

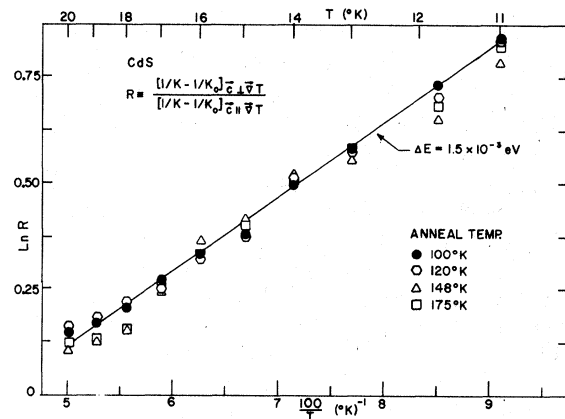


FIG. 8. Logarithm of the ratio of the additive thermal resistivities of CdS-c \perp to CdS-c \parallel as a function of reciprocal measuring temperature after annealing to the indicated anneal temperatures.

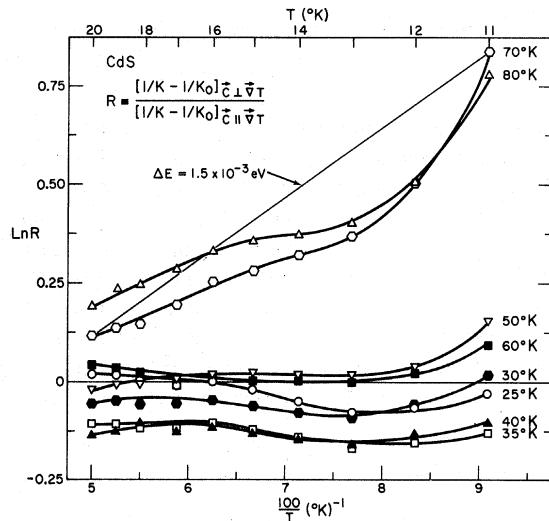


FIG. 9. Logarithm of the ratio of the additive thermal resistivities of CdS-cl to CdS-cll as a function of reciprocal measuring temperature after annealing to the indicated anneal temperatures.

$\ln R$ is very nearly 0, implying $R \approx 1$ for all temperatures, as expected if the additive thermal resistivity is isotropic. Between the anneal temperatures of 60 and 70 °K, however, a marked change takes place in R indicating that the additive thermal resistivity rapidly becomes anisotropic in this temperature range. We therefore conclude that the anisotropic defects are not present following irradiation but form upon annealing between 60 and 70 °K.

The advantage of the analysis in Fig. 9 is that it separates the effects of the anisotropic defects from the accompanying reverse and forward recovery of isotropic defects which are included in the data of Fig. 3.

C. Low-Temperature Motion of Primary Defects

The electron irradiations are believed to introduce primary defects (Cd and S interstitials and vacancies) into CdS in concentrations that are large compared with the impurity concentration. The almost complete annealing of the additive thermal resistivity below 300 °K suggests the almost complete annealing of these defects. The present results imply that certain primary defects begin to move in CdS at temperatures as low as 35 °K.

Recovery below room temperature is in agreement with the results of Bryant and Cox⁹ but in disagreement with the results of Chester.¹⁰ The fact that no recovery was observed by Chester between liquid-nitrogen temperature and room temperature suggests that primary defects were produced in concentrations smaller than the trap concentration, and that the complexes formed upon irradiation at liquid-nitrogen temperature remained

stable upon warming to room temperature.

The data in Fig. 3 show the existence of major annealing stages between 35 and 60, 60 and 100, and 175 and 270 °K. Between 60 and 70 °K, anisotropic defects are formed, and the concentration of the anisotropic defects greatly decreases above 175 °K. Since some of the anisotropic defects remain and are stable after annealing to room temperature as indicated in Figs. 3-5, the anisotropic defects presumably are attacked by primary defects which become mobile above 175 °K. Recently, Randolph and Oswald²³ have observed the almost complete recovery near 200 °K of an exciton spectra produced by ⁶⁰Co x rays at 78 or 4.2 °K.

The most definitive information that exists on the nature of primary defects in CdS are the results of investigations of the luminescent centers. Luminescent bands have been observed in CdS upon electron bombardment at 5200, 6050, 7200 Å, and 1.04 μ. For a compound such as CdS where the atomic weights of the constituents are quite different, it can be expected that two distinct thresholds for displacements would be observed, the lower-energy threshold representing displacement of the sulfur atom, and the higher-energy threshold representing displacement of the heavier cadmium atom. Kulp and Kelley⁷ observed a threshold for displacement in CdS at 115 keV. Above this energy, bombardment by electrons at room temperature produced the bands at 5200 and 7200 Å. These were attributed to defects involving the sulfur interstitial and the sulfur vacancy, respectively. For electron irradiation at liquid-nitrogen temperature, a higher threshold of 290 keV was observed, above which two additional bands at 6050 Å and 1.04 μ were produced upon irradiation. These two bands have been assigned to defects which involve the Cd interstitial and the Cd vacancy, respectively.

For 275-keV electron irradiation at liquid-nitrogen temperature of a sample exhibiting all four luminescences prior to bombardment, Kulp⁸ observed that the green-edge emission at 5200 Å continuously increases on bombardment, whereas the luminescence at 7200 Å continuously decreases. The other bands saturate and remain constant. We conclude from this that the sulfur interstitial assigned to the green-edge emission (5200 Å) is mobile upon irradiation at liquid-nitrogen temperature and partially recovers the 7200-Å center which contains a sulfur vacancy. If the electron-beam energy is raised to 300 keV, the band at 1.04 μ and the bands at 6050 and 5200 Å increase in intensity with bombardment, and the 7200-Å band continues to decrease in intensity. Annealing to room temperature following bombardment shows partial recovery of all of the bands.

The threshold results imply that 2-MeV electron irradiation of CdS produces both sulfur and cadmium

interstitials and vacancies. If the luminescence results are interpreted to indicate that sulfur interstitials move at liquid-nitrogen temperature and sulfur vacancies are not sufficiently mobile to form additional 7200-Å centers, then we suggest that the anisotropic defects are formed by the trapping of sulfur interstitials, possibly at the cadmium vacancies. Cadmium vacancies may also exist before irradiation in sulfur-compensated crystals such as these. For such a model the sulfur interstitial could have two positions, either along the *c* axis or at approximately 60° in three equivalent directions from the *c* axis. The small equilibrium energy difference of orientation that is observed seems consistent with such a model.

Since monovacancies in the II-VI semiconductors are believed to move on their own sublattice, they can be expected to be more stable than vacancies in the elemental semiconductors. Recent electron paramagnetic resonance (EPR) results confirm this belief for the Zn vacancy in ZnSe,²⁴ and it is stable at room temperature. The recovery near 200°K in CdS could then be assigned to the motion of the Cd interstitial. It would be important to check these suggestions by studies of the development and polar-

ization of the luminescent centers upon electron irradiation at low temperature. In preliminary experiments, Fraley and Kulp²⁵ have found an electron irradiation induced decrease in bound-exciton emission which anneals out near 240°K. The electron-bombardment energy threshold for the production of the luminescence decrease is associated with the Cd-threshold displacement energy,²⁵ in agreement with the proposed model.

The suggestion of very mobile interstitials in CdS is similar to the interpretation of results which suggest that highly mobile interstitials exist in the elemental semiconductors germanium and silicon.¹ Furthermore, for CdS in particular, Woodbury and Hall,²⁶ and Woodbury²⁷ have concluded that neutral interstitials are the important diffusing defects and that the mechanism for establishing chemical equilibrium is dominated by the neutral interstitials over most of the solidus region.

ACKNOWLEDGMENTS

It is a pleasure to acknowledge the competent technical assistance of H. J. Smalley in the conduction of the experiments and to thank H. J. Stein for valuable suggestions on the manuscript.

†Work supported by the U. S. Atomic Energy Commission.

¹See, e.g., J. W. Corbett in *Radiation Effects in Semiconductors*, edited by F. L. Vook (Plenum, New York, 1968), p. 3; also J. H. Crawford, Jr., *ibid.*, p. 469.

²The optical properties of II-VI semiconductors have been reviewed by D. C. Reynolds, C. W. Litton, and T. C. Collins, *Phys. Status Solidi* **12**, 3 (1965); **9**, 645 (1965).

³N. A. Vlasenko, N. I. Vitoikhovskii, F. L. Denisova, and V. F. Pavlenko, *Opt. i Spectroskopiya* **21**, 261 (1966) [*Opt. Spectry. (USSR)* **21**, 466 (1966)].

⁴The results of recent research are contained in *II-VI Semiconducting Compounds*, edited by D. G. Thomas (Benjamin, New York, 1967).

⁵O. Goede and E. Gutsche, *Phys. Status Solidi* **17**, 911 (1966).

⁶R. J. Collins, *J. Appl. Phys.* **30**, 1135 (1959).

⁷B. A. Kulp and R. H. Kelley, *J. Appl. Phys.* **31**, 1057 (1960).

⁸B. A. Kulp, *Phys. Rev.* **125**, 1865 (1962); in *Radiation Damage in Semiconductors*, edited by P. Baruch (Dunod Cie., Paris, 1964), p. 173.

⁹F. J. Bryant and A. F. J. Cox, *Proc. Roy. Soc. (London)* **A310**, 319 (1968).

¹⁰R. O. Chester, *J. Appl. Phys.* **38**, 1745 (1967).

¹¹Preliminary reports of some of this work were given in F. L. Vook, *Bull. Am. Phys. Soc.* **13**, 359 (1968);

Appl. Phys. Letters **13**, 25 (1968).

¹²F. L. Vook, *Phys. Rev.* **135**, A1742 (1964).

¹³F. L. Vook, *Phys. Rev.* **135**, A1750 (1964); **149**, 631 (1966).

¹⁴F. L. Vook, *Phys. Rev.* **138**, A1234 (1965).

¹⁵F. L. Vook, *Phys. Rev.* **140**, A2014 (1965).

¹⁶G. E. Moore, Jr. and M. V. Klein, *Phys. Rev.* **179**, 722 (1969).

¹⁷M. G. Holland, *Phys. Rev.* **134**, A471 (1964).

¹⁸H. B. Im and R. H. Bube, *J. Appl. Phys.* **39**, 2908 (1968); *Bull. Am. Phys. Soc.* **13**, 380 (1968).

¹⁹P. Erdős, *Phys. Rev.* **138**, A1200 (1965); P. Erdős and S. B. Haley, *ibid.* **184**, 951 (1969).

²⁰A. E. Kazakov and E. L. Nagaev, *Fiz. Tverd. Tela* **8**, 2878 (1966) [*Soviet Phys. Solid State* **8**, 2302 (1967)].

²¹H. J. Albany and M. Vandevyver, *J. Appl. Phys.* **38**, 425 (1967).

²²M. Moss, *J. Appl. Phys.* **36**, 3308 (1965).

²³L. P. Randolph and R. B. Oswald, Jr., *Bull. Am. Phys. Soc.* **15**, 398 (1970).

²⁴G. D. Watkins, *Rad. Eff.*, (to be published).

²⁵P. E. Fraley and B. A. Kulp, *Bull. Am. Phys. Soc.* **13**, 380 (1968); (private communication).

²⁶H. H. Woodbury and R. B. Hall, *Phys. Rev.* **157**, 641 (1967).

²⁷H. H. Woodbury, in *II-VI Semiconducting Compounds*, edited by D. G. Thomas (Benjamin, New York, 1967), p. 244.